PAPER

Check for updates

Imidazolyl activated carbon refluxed with ethanediamine as reusable heterogeneous catalysts for Michael addition

Wenzhu Liu, [ID] [a] Jiafu Xiao, [ID] [a] Qiong Xu,*[a] Xianxiang Liu, [ID] [a] Sheng Zhong,[b] Hua Huang,[b] Min Zheng,[c] Steven Robert Kirk [ID] [a] and Dulin Yin*[a]

Imidazolyl activated carbon, denoted as AC-N, was prepared *via* oxidation of AC with HNO_3 (AC-O) and then refluxed with ethanediamine under mild conditions. The results showed that the N content of AC-N was 10.3%, and the surface alkali group density of AC-N was 0.96 mmol g^{-1} from 0.78 mmol g^{-1} carboxy group of AC-O by Boehm titration. It was revealed that the basic functional groups on the AC-N surface included imidazole and amine groups, from XPS and FT-IR. Evaluated with Michael addition of furfural, the catalytic performance of AC-N showed higher conversion and selectivity than that of commonly used base catalyst such as 2-methylimidazole and KOH. Very remarkably, AC-N showed extraordinary recyclability, in that there was no decline of conversion and selectivity after being recycled 5 times.

1. Introduction

Activated carbon (AC) materials are known to have a highly developed pore structure, large specific surface area, changeable surface chemical characteristics and high surface activity,[1,2] and have been widely used in adsorption,[3–7] catalysis[8,9], electrode materials[10], and decoloration,[11] *etc.* It's been believed that the most attractive property of activated carbon materials is their controllable surface properties, with controlled amounts of aromatic rings and oxygen-containing functional groups. Acidic surface sites on AC have usually been generated by treatments in liquid media with oxidative agents such as HNO_3,[12–14] H_2SO_4,[15] $(NH_4)_2S_2O_8$[16] and $KMnO_4$.[17] An alkali surface of activated carbon is enormously in demand in extensive specific areas and has attracted many researchers' interest. There were a number of studies related to the preparation of activated carbons by steeping or reaction with KOH and NaOH.[18–20] Park[21] prepared basic activated carbons with coconut shell AC in NaOH solution, and the surface pH was 10.2. Cazetta[22] prepared alkaline surface activated carbon by mixing coconut shell char with NaOH and the basic density was 0.73–0.75 mmol g^{-1}.

In recent years, some meaningful explorations found that an alkaline surface could be constructed by treating activated carbons with ammonia or amines, while the procedures known

to make active carbon surfaces basic usually involved treatment under high temperatures. Barbosa[23] prepared carbon dots from cow manure and functionalized them with ethylenediamine, affording amide bonds that resulted in bright green fluorescence, which improved cellular selectivity for nucleoli staining. Gao[24] prepared a series of mesoporous, N-containing carbon materials directly from pure chitin by means of carbonization at 400–1000 °C enriched with amine, amide, and pyrrolic functionalities. Li[25] prepared nitrogen-doped activated carbons utilizing agricultural waste (corncob) as precursor under N_2 flow with NH_3 as a nitrogen source under 400–600 °C, the N content was 2.97 wt% to 3.98 wt%. Wang[26] prepared N-doped hierarchical porous carbon with urea at 180 °C in an autoclave and then immersed in potassium hydroxide solution: in this case, the N content was around 2.5%. Lahaye[27] provided activated carbon fibers with a basic surface by treatment with ammonia at 500–800 °C and the N content of the products was 0.94–4.06%. Stöhr[28] proposed that amination of activated carbons lead to the formation of NH_2 or NH functional groups attached to the carbon rings at 600–900 °C. Park[29] prepared mesoporous nitrogen-doped activated carbon with (1-methyl-1*H*-pyrrole-2-yl) methanol and KOH at 100–850 °C, where the majority of the N was assigned to pyridinic and graphitic nitrogen. Seredych[30] explanted amine functional groups on wood-origin activated carbon with oxidation by 50% HNO_3 and then treated with melamine and urea followed by carbonization at 950 °C in an inert atmosphere, and the density of basic surface groups was 0.688 mmol g^{-1}. Kan-Nari[31] doped nitrogen to activated carbon by treating in a stream of mixture of ammonia and air at temperatures of 400–800 °C and used it as alkaline catalyst in a Knoevenagel condensation and transesterification. Watanabe[11] and Fujita[32] prepared nitrogen-doped activated carbon

[a]National and Local Joint Engineering Laboratory for New Petro-Chemical Materials and Fine Utilization of Resources, College of Chemistry and Chemical Engineering, Hunan Normal University, 410081, Changsha, China. E-mail: xuqiong@hunnu.edu.cn; dulinyin@126.com; Tel: +86 18942513809; +86 13808496387

[b]Hunan Changling Petrochemical S & T Developing Co. Ltd, 414012, Yueyang, China

[c]Hunan First Normal University, 410205, Changsha, China

via treatments of activated carbon with H_2O_2 and then ammonia at temperatures of 600–800 °C and the N were pyridine-, pyrrole-, and graphite-type nitrogen species.

Michael reaction with nitroalkanes is one of the most important reactions for formation of a carbon–carbon bond, involving the nucleophilic addition of a carbanion to α,β-unsaturated carbonyl compounds, and is base-catalysed.[33] In recent years, a variety of solid base catalysts has been reported, including potassium carbonate,[34] amines anchored at surfaces,[35] organic resins,[36] KF supported on α-Al_2O_3,[37] and KF supported on hydrotalcite.[38] A major drawback of some catalysts is that their use resulted in the increased formation of secondary products in the reactions. Reusable of the catalyst has seldom been demonstrated, which represents a severe limitation to its practical use.

In this work, we reported a convenient route (without high temperature and pressure) to construct an alkaline surface from the acidic activated carbon, with large amounts of nitrogen-containing groups, under the refluxed conditions with ethylenediamine at 117 °C, and the catalytic performance and reusable ability of AC-N on Michael additions was studied.

2. Experimental

2.1 Surface modification of activated carbon

In general, 10 g activated carbon was added to 150 mL 12 mol L^{-1} HNO_3 in a three-necked flask connected with a condenser and thermometer, and stirred at 80 °C for 8 hours. After completion of the reaction, the reaction mixture was filtered, washed with water and ethanol, and then dried. The oxidized activated carbon was denoted as AC-O. The AC-O was added into 150 mL ethylenediamine and refluxed at 117 °C for 8 hours. The mixture was filtered, washed with water and alcohol, and then AC-N was prepared after drying.

2.2 Sample characterization

2.2.1 Density of acid. The density of acid was quantified by Boehm titration.[39] 50 mg AC-O was added into 20 mL 0.01 mol L^{-1} $NaHCO_3$ and sonicated for 30 min. After filtering and washing with distilled water, the filtrate was titrated with 0.01 mol L^{-1} HCl using bromocresol green–methyl red mixed indicator as the indicator.

2.2.2 Density of alkali. 50 mg AC-N was added into 20 mL 0.01 mol L^{-1} HCl and sonicated for 30 min. After it was filtered and washed with distilled water, the filtrate was titrated with 0.01 mol L^{-1} NaOH using phenolphthalein as the indicator.

2.2.3 Elemental analysis. The content of N analysis was analysed with vario EL III Elemental analyser (Germany). The tested conditions were: oxidation furnace temperature 1150 °C, carrier gas (He) flow 200 mL min^{-1}, oxygen flow 200 mL min^{-1}, combustion time 90 s.

2.2.4 Determination of specific surface area. The surface properties and surface area of the samples were characterized by N_2 adsorption measurements at 77 K using a surface area analyzer (TriStar 3000). The surface area (S_{BET}) was calculated from isotherms using the Brunauer–Emmett–Teller (BET)

equation. The volume of liquid nitrogen corresponding to the amount adsorbed at a relative pressure of $P/P_0 = 0.99$ was defined as the total pore volume.

2.2.5 Thermogravimetric (TG). In order to plot TG and DTG curves for samples, NETZSCH STA 409 PC/PG thermal gravimetric analyzer was used. 20 mg samples were heated, starting at room temperature and reaching up to 800 °C by increasing the temperature 10 °C min^{-1} gradually under N_2.

2.2.6 Fourier transforms infrared (FT-IR). FT-IR spectroscopy analysis was performed using a Perkin Elmer 283 spectrometer. The samples for FT-IR analyses were prepared by mixing them with KBr powder and pressing the mixture into pellets. The FT-IR spectra were recorded between 4000 and 400 cm^{-1} (with a resolution of 4 cm^{-1} and acquisition rate of 20 scan per min).

2.2.7 X-ray photoelectron spectroscopy (XPS). A K-Alpha 1063 X-ray Photoelectron Spectrometer system was operated in a constant-pass energy mode at 50 eV with a step size of 0.100 eV. Survey scans in the range of 10 to 1350 eV were recorded. Prior to analysis, samples were dried at 105 °C and then kept under vacuum.[40,41]

2.3 Catalytic performance test

The catalytic performance of AC-N in catalyzing the Michael addition reaction was tested. In general, a certain amount of substrates was added into a three-necked flask equipped with a thermometer and condenser. The effects of different temperature, time, and the catalyst amount on furfural conversion rate and 3-(nitromethyl)-2,3-dihydrofuran-2-carbaldehyde selectivity were investigated. Different catalysts were used for comparation with AC-N in furfural Michael addition, and various substrates were used for testing the applicability of AC-N.

3. Results and discussion

3.1 Structure and texture for AC-N

3.1.1 Nitrogen adsorption–desorption studies. Surface areas of AC-O and AC-N were determined by means of the standard BET equation. The nitrogen adsorption–desorption curves are shown in Fig. 1. The N_2 adsorption isotherm of the samples belonged to the type IV class of adsorption isotherm,
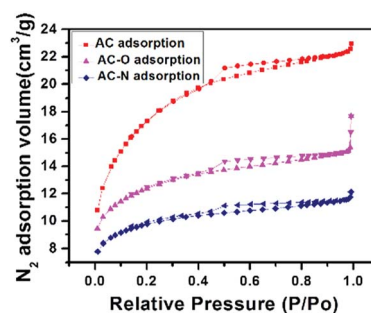

Fig. 1 N_2 adsorption–desorption isotherms for parent AC, AC-O and AC-N.

which indicates the presence of a uniform mesoporous structure.[29] At higher relative pressure, the adsorption capacity increased with the increase of the relative pressure. The adsorption isotherm showed an upturned "tail", and gradually intersects with the relative pressure $p/p_0 = 1$ axis, and desorption curves showed an obvious hysteresis loop, indicating that the three samples also had mesoporous structure. Fig. 2 shows results from the pore size distribution measurements for the samples. The results showed that oxidation of the carbon resulted in the decrease in the degree of mesoporous structure for AC-O and AC-N sample compared to AC. This is as a result of pore blockage in the mesoporous structure during the oxidation process. The porous structures of samples were shown in Table 1. After oxidation, the specific surface area of AC-O decreased to 614 m^2 g^{-1} from 1286 m^2 g^{-1} of AC, and the pore volume simultaneously decreased to 0.38 cm^3 g^{-1} from 0.77 cm^3 g^{-1}, which was due to the blocking of the pores by the surface complexes introduced by nitric acid treatment.[7] After amination, the surface area of AC-N decreased to 418 m^2 g^{-1}, and the pore volume also decreased to 0.26 cm^3 g^{-1}, while the most probable pore size remained basically unchanged for the three carbon materials.

3.1.2 FT-IR. The FT-IR spectra of AC, AC-O, AC-N and AC mixed with 2-methylimidazole were shown in Fig. 3. It can be seen that the spectra showed a number of adsorption peaks, indicating the complex nature of the samples. In all samples, a strong absorption band was observed at around 3400 cm^{-1} and this was assigned to carboxylic group O–H stretching.[2] In the spectrum of AC, the absorption at 1720 cm^{-1} was attributed carboxylic acid group, which was also found in the sample AC-O. In the samples AC and AC-O, the peaks at 1600 cm^{-1} were attributed to a quinone structure.[7] The weak peaks around 1260 to 1060 cm^{-1} are due to the C=C stretching that can be
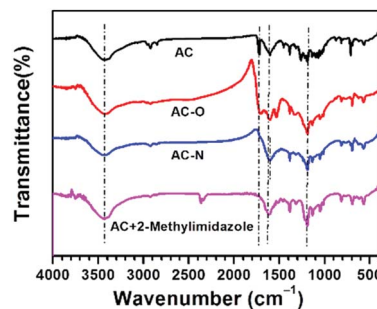

Fig. 3 FT-IR spectra for the AC, AC-O and AC-N.

attributed to the presence of aromatic rings in AC. After oxidation, the weak peaks around 1260 to 1060 cm^{-1} disappeared, which indicated that oxidization process destroyed the C=C on the AC surface. In all the samples except AC, the broad peak around 1200 cm^{-1} may be attributed to different functional groups containing single-bonded oxygen atoms such as phenols, ethers, and lactones,[6] or single-bonded nitrogen atoms such as C–N, –NH and –NH$_2$.[2,7,10] For the sample AC-N, there were no absorption peaks at 1720 and 1600 cm^{-1}, while a new absorption peak appeared at 1604 cm^{-1}, which was attributed to C–N stretching vibration.[10] The absorption of the N–H stretching vibration also appeared at around 3400 cm^{-1}, which nearly overlapped with that of O–H stretching. The FT-IR spectra of AC mixed with 2-methylimidazole was indistinguishable from that of AC-N, which indicated that N-containing groups on the surface of AC-N were similar to the structure of 2-methylimidazole.

3.1.3 Density of acid and alkali. Density of acid and alkali in AC, AC-O and AC-N were measured by Boehm titration: the results were shown in Table 1. The texture parameters of the material are also shown in Table 1. These results indicated that there was absolutely no acidic center and alkali center on the AC surface, while certain H$^+$ acidic centers were detected in AC-O. After the amination with ethylenediamine, the acidic center on AC-O surface, carboxyl groups were completely destroyed and converted to basic centers.

3.1.4 Elemental analysis. The contents of nitrogen in AC, AC-O and AC-N were analyzed with elemental analyzer. The results were shown in Table 1. As shown, N content of AC-O was slightly lower than that of AC caused by oxidization. After treated with ethanediamine, the N content of AC-N was increased to 10.3%, which indicated that N-contained group was grafted on carbon successfully.
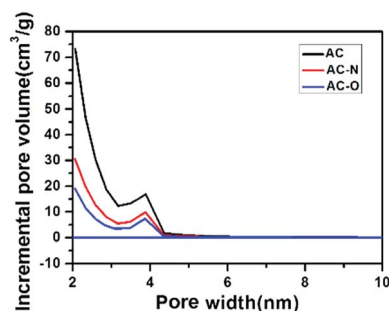

Fig. 2 Pore size distribution for the samples.

Table 1 The surface acid–base properties and texture features of samples

Samples	c_{H^+} (mmol g^{-1})	$^a c_{NA}$ (mmol g^{-1})	^{b}N content (%)	^{c}N content (%)	BET surface area (m^2 g^{-1})	Pore volume (cm^3 g^{-1})	Pore size (nm)
AC	0.03	0.00	0.26	0.56	1286	0.77	2.4
AC-O	0.78	0.00	0.23	0.35	614	0.38	2.5
AC-N	0.00	0.96	9.38	10.3	418	0.26	2.5

^{a} c_{NA} represents for concentration of alkali site caused with N. ^{b} N represents for N content analyzed with XPS. ^{c} N represents for N content analyzed with elemental analyzer.

3.1.5 XPS. To understand the surface chemistry of AC-N, the nature of C, O and N species at the surface of different samples (including AC-N, AC-N mixed with 2-methylimidazole and AC mixed with ethylenediamine) were investigated by XPS. The survey spectra were shown in Fig. 4, and the C1s and N1s XPS spectra are shown in Fig. 5. As shown, the C1s of AC mainly consisted with features at 284.8, 286.1 and 287.9 eV, corresponding to sp^2 C, C–O (C–N) and C=O (C=N) groups,[6,29] respectively. For AC-N, the peaks at 286.1 and 287.9 eV were enhanced after the oxidation and amination of AC, which indicated that the surface functional groups changed a little during the treatment of AC. The N1s peaks of AC-doped methyl imidazole mainly consist of three peaks, which were located at 398.7, 399.5 and 401.4 eV, respectively, corresponding to pyridine-type (C–N=C), pyrrole-type (C–NH–C) and graphite-type nitrogen.[9,11,30,31,35] As expected, after modification of AC to AC-N, the corresponding N1s peaks in methylimidazole were shifted 0.2 eV towards the low energy region, which indicated that a certain amount of imidazole structure existed in AC-N. A strong peak appeared at 400.1 eV in AC-N, corresponding to the nitrogen in C–NH$_2$,[31] indicating that some of the amino groups in AC-N did not dehydrate to form a ring.
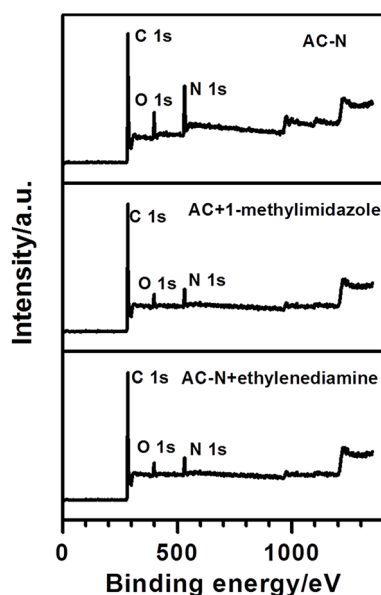

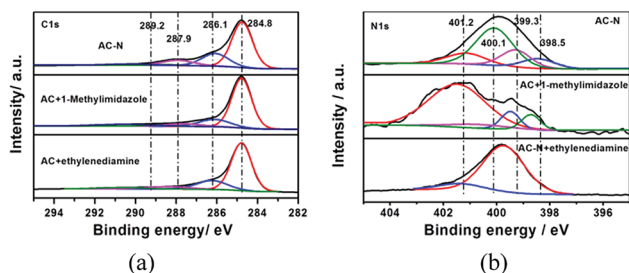Fig. 4 Survey of AC-N and AC mixed with 2-methylimidazole and ethylenediamine.

Fig. 5 C1s (a) and N1s (b) XPS spectra of AC-N, AC mixed with 2-methylimidazole and AC mixed with ethylenediamine.

3.1.6 TG-DTG. The thermal stability of the different samples was determined by TG-DTG and depicted in Fig. 6. The thermogravimetric analysis (TG) weight loss stages were observed in all samples. A significant weight loss below 100 °C can be attributed to elimination of the adsorbed water: it was notable that the water-loss temperature of AC-O (103.5 °C) and AC-N (98.7 °C) was higher than AC (78.3 °C), indicating a higher affinity for water. The weight-loss peak at 350 °C was present in AC-N, which was higher than that of in AC-O (306 °C), while there was no peak presented in sample AC. The differences are mainly caused by the organic components generated by oxide and alkaline modification processes, which also showed that the alkaline function groups were more stable than acidic oxygen functional groups. According to Fig. 6, hydrophilic groups were generated on the AC surface in the oxidation process, while the surface structure was damaged at a certain degree at the edge of the structure to produce a certain amount of components which were easily decomposed. After amination, the peak of water loss was lower than that of AC-O, and the other weight-loss peak was increased, which indicated that the surface structure of AC-N was further changed and the hydrophilicity was slightly lower than that of AC-O. The thermal stability of the new component was enhanced to a certain extent.

According to the texture and spectrum analysis of AC, AC-O and AC-N, the surface groups of the material were shown as Fig. 7. After oxidation, the content of oxygen-containing functional groups on the AC-O surface was increased, including carboxyl groups, hydroxyl groups, carbonyl groups, lactone groups and so on. After amination treatment, the carboxyl group on AC-O surface reacted with ethylenediamine to form an amide structure, and further dehydration into the ring occurred to form a similar imidazole structure. Part of carbonyl group reacted with ethylenediamine to form an amino group in the surface of AC-N.

3.2 Catalyst performances

3.2.1 The catalytic performance of AC-N on furfural Michael additions. Michael addition is a very efficient, high
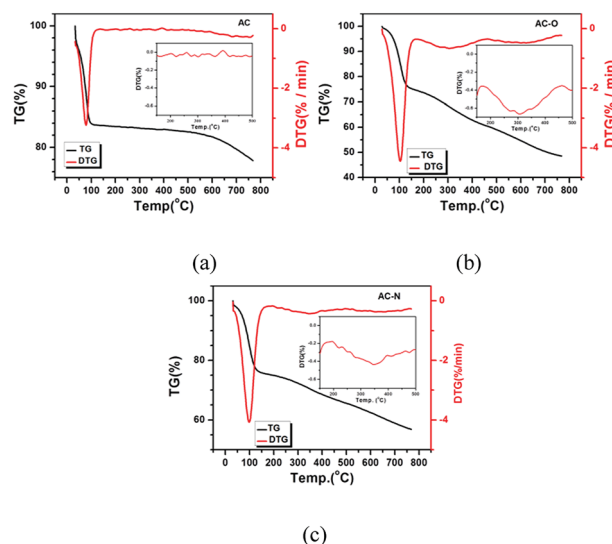

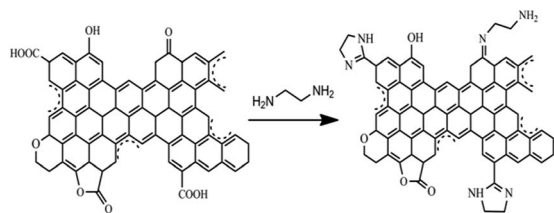Fig. 6 TG and DTG analysis of (a) AC; (b) AC-O; (c) AC-N.

Fig. 7 Scheme of preparing AC-N.

Fig. 10 Reusability of AC-N for Michael addition of furfural.

atom economy carbon–carbon formation reaction in organic synthesis, so the development of the Michael addition reaction has attracted the attention of organic chemists for the past several decades. In this work, the Michael addition reaction was studied using AC-N as a solid base catalyst. The reaction scheme was shown in Fig. 8.

The effects of temperature, time, and catalyst dosage on the conversion of furfural and the selectivity of 3-(nitromethyl)-2,3-dihydrofuran-2-carbaldehyde were investigated. From the results in Fig. 9, it can be seen that the conversion of furfural and the selectivity of 3-(nitromethyl)-2,3-dihydrofuran-2-carbaldehyde were not changed at different temperatures when the reaction time was 7 h. Neither of the conversion and the selectivity changed when the temperature was above 120 °C. Therefore, the reaction conditions were chosen as 120 °C with a reaction time of 7 h. When the amount of catalyst was less than 2.0 mol%, the conversion of furfural and the selectivity of 3-(nitromethyl)-2,3-dihydrofuran-2-carbaldehyde increased with the amount of catalyst. When the amount of the catalyst was more than 2.0 mol%, neither of these was changed.

3.2.2 Catalyst reusability. One of the main advantages of heterogeneous solid catalysts is that they can be easily recovered from the reaction mixture and can be regenerated for reuse. In the present study, the catalyst AC-N was washed thoroughly with ethanol, followed by vacuum drying for 12 h. The catalyst was then reused for the next run under the same reaction

Table 2 Effect of different catalysts and substrates on Michael addition[a]

Catalysts	Substrates	Time (h)	Conv. (%)	Sel. (%)
None	Furfural	10	1	70
2-Methylimidazole	Furfural	10	23	77
KOH	Furfural	10	54	60
Cs_2CO_3	Furfural	10	46	62
CaO	Furfural	10	35	58
AC-N	Furfural	7	87	99
AC-N	Citral	7	93	93
AC-N	Crotonaldehyde	7	96	99
AC-N	trans-2-Pentenal	7	96	99
AC-N	3-Methyl-2-butenal	7	95	97

[a] Reaction conditions: mol (nitromethane/aldehyde) = 3, catalyst 2 mol%, 120 °C.

conditions. As shown in Fig. 10, after 5 cycles, the conversion and selectivity of furfural remained unchanged at 87% and 99% respectively, which means excellent stability of the catalyst on furfural in the Michael addition reaction.

3.2.3 Catalysts comparison for furfural Michael addition and substrates applicability catalyzed with AC-N. The effect of commonly used catalysts on the reaction of furfural with nitromethane were studied and compared with that of AC-N. The results were shown in Table 2. According to Table 2, the conversion of furfural was 87% and the selectivity of the 3-(nitromethyl)-2,3-dihydrofuran-2-carbaldehyde was 99% catalyzed with AC-N. Under the same conditions, the conversion of furfural was 54%, 46%, 35% and the selectivity of 3-(nitromethyl)-2,3-dihydrofuran-2-carbaldehyde was 60%, 62%, 58% using KOH, Cs_2CO_3, CaO as inorganic base catalysts, respectively. The conversion of furfural was only 23% and the selectivity of the 3-(nitromethyl)-2,3-dihydrofuran-2-carbaldehyde was 77% using methylimidazole as catalyst. The experimental results showed that AC-N expressed better catalytic performance than those commonly used base catalyst. As a solid catalyst, AC-N had the advantage of being easily separated from the reaction system. With AC-N as a catalyst, the Michael addition of different substrates was studied. As shown in Table 2, AC-N showed better catalysis performance in chain olefine aldehyde.
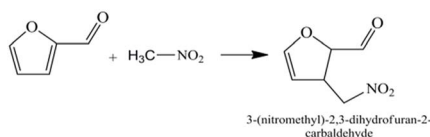

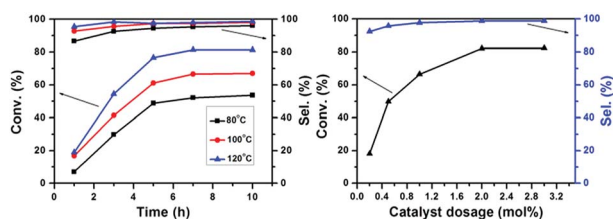Fig. 8 Michael reaction of nitromethane on furfural.

Fig. 9 Effect of temperature, time, and catalyst dosage on conversion of furfural and selectivity of 3-(nitromethyl)-2,3-dihydrofuran-2-carbaldehyde.
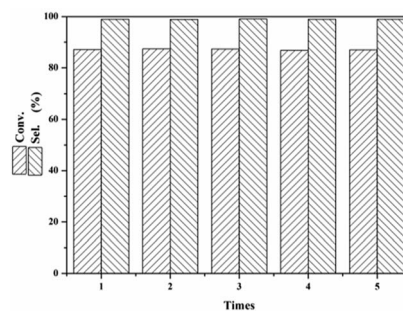
4. Conclusions

A new activated carbon material containing a certain amount of imidazole groups and amine groups on surface was prepared *via* oxidation using HNO_3 and then amination using ethanediamine under atmospheric pressure with activated carbon as a raw material. Compared with the related previously-published research reports, the route reported in this research avoided treatment at high temperature and high pressure. The structure analysis showed that AC-N contained a certain amount of imidazole structure and the results showed that the N content of AC-N was 10.3%. The surface alkali density of the material was 0.96 mmol g^{-1} and the specific surface area was 418 $m^3 g^{-1}$.

As a solid base catalyst, AC-N showed an excellent catalytic performance on the Michael addition reaction of furfural, which was better than that of 2-methylimidazole, a homogeneous alkaline catalyst, and also better than that of inorganic strong base KOH under the same conditions. After 5 cycles, the conversion of furfural remained at around 87% and the selectivity was 99% of 3-(nitromethyl)-2,3-dihydrofuran-2-carbaldehyde, which means excellent stability of the catalyst on furfural for the Michael addition reaction.

Conflicts of interest

There are no conflicts to declare.

Acknowledgements

References

1 T. M. Alslaibi, I. Abustan, M. A. Ahmad and A. A. Foul, *J. Chem. Technol. Biotechnol.*, 2013, **88**, 1183–1190.

2 P. Chingombe, B. Saha and R. J. Wakeman, *Carbon*, 2005, **43**, 3132–3143.

3 S. W. Nam, D. J. Choi, S. K. Kim, N. Her and K. D. Zoh, *J. Hazard. Mater.*, 2014, **270**, 144–152.

4 S. Haydar, M. A. Ferro-GarcíA, J. Rivera-Utrilla and J. P. Joly, *Carbon*, 2003, **41**, 387–395.

5 Y. F. Jia, A. B. Xiao and K. M. Thomas, *Langmuir*, 2002, **18**, 470–478.

6 J. P. Chen and S. Wu, *Langmuir*, 2004, **20**, 2233–2242.

7 J. W. Shim, S. J. Park and S. K. Ryu, *Carbon*, 2001, **39**, 1635–1642.

8 W. Qi and D. Su, *ACS Catal.*, 2014, **4**, 415–429.

9 M. Kubota, A. Hata and H. Matsuda, *Carbon*, 2009, **47**, 2805–2811.

10 Y. Liu, Z. Hu, K. Xu, X. Zheng and Q. Gao, *Acta Phys.-Chim. Sin.*, 2008, **24**, 1143–1148.

11 H. Watanabe, S. Asano, S. Fujita, H. Yoshida and M. Arai, *ACS Catal.*, 2015, **5**, 2886–2894.

12 J. J. Ternero-Hidalgo, J. M. Rosas, J. Palomo, M. J. Valero-Romero, J. Rodríguez-Mirasol and T. Cordero, *Carbon*, 2016, **101**, 409–419.

13 N. Wibowo, L. Setyadhi, D. Wibowo, J. Setiawan and S. Ismadji, *J. Hazard. Mater.*, 2007, **146**, 237–243.

14 R. R. V. A. Rios, D. E. Alves, I. Dalmázio, S. F. V. Bento, C. L. Donnici and R. M. Lago, *Mater. Res.*, 2003, **6**, 129–135.

15 M. A. Álvarez-Merino, V. López-Ramón and C. Moreno-Castilla, *J. Colloid Interface Sci.*, 2005, **288**, 335–341.

16 G. Yadavalli, H. Lei, Y. Wei, L. Zhu, X. Zhang, Y. Liu and D. Yan, *Biomass Bioenergy*, 2017, **98**, 53–60.

17 A. A. Daifullah, S. M. Yakout and S. A. Elreefy, *J. Hazard. Mater.*, 2007, **147**, 633–643.

18 D. Lozano-Castelló, M. A. Lillo-Ródenas, D. Cazorla-Amorós and A. Linares-Solano, *Carbon*, 2001, **39**, 741–749.

19 H. Teng and L. Y. Hsu, *Ind. Eng. Chem. Res.*, 1999, **38**, 2947–2953.

20 T. Otowa, Y. Nojima and T. Miyazaki, *Carbon*, 1997, **35**, 1315–1319.

21 S. J. Park and Y. S. Jang, *J. Colloid Interface Sci.*, 2002, **249**, 458–463.

22 A. L. Cazetta, A. M. M. Vargas, E. M. Nogami, M. H. Kunita, M. R. Guilherme, A. C. Martins, T. L. Silva, J. C. G. Moraes and V. C. Almeida, *Chem. Eng. J.*, 2011, **174**, 117–125.

23 C. D. E. S. Barbosa, J. R. Corrêa, G. A. Medeiros, G. Barreto, K. G. Magalhaes, A. L. Oliveira, J. Spencer, M. O. Rodrigues and B. A. D. Neto, *Chem.–Eur. J.*, 2015, **21**, 5055–5060.

24 Y. J. Gao, X. Chen, J. G. Zhang and N. Yan, *ChemPlusChem*, 2015, **80**, 1556–1564.

25 B. Li, F. Dai, Q. F. Xiao, L. Yang, J. M. Shen, C. M. Zhang and M. Cai, *Energy Environ. Sci.*, 2016, **9**, 102–106.

26 W. Wang, H. Quan, W. Gao, R. Zou, D. Chen, Y. Dong and L. Guo, *RSC Adv.*, 2017, **27**, 16678–16687.

27 J. Lahaye, G. Nansé, A. Bagreev and V. Strelko, *Carbon*, 1999, **37**, 585–590.

28 B. Stöhr, H. P. Boehm and R. Schlögl, *Carbon*, 1991, **29**, 707–720.

29 J. Park, Y. Nabae, T. Hayakawa and M. Kakimoto, *ACS Catal.*, 2014, **4**, 3749–3754.

30 M. Seredych, D. Hulicova-Jurcakova, Q. L. Gao and T. J. Bandosz, *Carbon*, 2008, **46**, 1475–1488.

31 N. Kan-Nari, S. Okamura, S. I. Fujita, J. I. Ozaki and M. Arai, *Adv. Synth. Catal.*, 2010, **352**, 1476–1484.

32 S. I. Fujita, H. Watanabe, A. Katagiri, H. Yoshida and M. Arai, *J. Mol. Catal. A: Chem.*, 2014, **393**, 257–262.

33 H. Guo, X. Li, J. L. Wang, X. H. Jin and X. F. Lin, *Tetrahedron*, 2011, **42**, 8300–8303.

34 G. Bosica and K. Polidano, *J. Chem.*, 2017, **2017**, 6267036.

35 A. Corma, S. Iborra, I. Rodriguez, M. Iglesias and F. Sanchez, *Catal. Lett.*, 2002, **82**, 237–242.

36 R. Ballini, P. Marziali and A. Mozzicafreddo, *J. Org. Chem.*, 1996, **61**, 3209–3211.

37 J. M. Clacens, D. Genuit, L. Delmotte, A. G. Ruiz, G. Bergeret, R. Montiel, J. Lopez and F. Figueras, *J. Catal.*, 2004, **221**, 483–490.

38 B. M. Choudary, B. Kavita, N. S. Chowdari, B. Sreedhar and M. L. Kantam, *Catal. Lett.*, 2002, **78**, 373–377.

39 I. Ogino, Y. Suzuki and S. R. Mukai, *Catal. Today*, 2018, **314**, 62–69.

40 C. L. Mangun, K. R. Benak, J. Economy and K. L. Foster, *Carbon*, 2001, **39**, 1809–1820.

41 R. J. J. Jansen and H. V. Bekkum, *Carbon*, 1995, **33**, 1021–1027.